Adsorption characteristics of Fe(III) and Fe(III)–NTA complex on granular activated carbon

D.S. Kim*

Department of Environmental Science and Engineering, Ewha Womans University, Daehyundong 11-1, Seodaemungu, Seoul 120-750, South Korea

Abstract

The adsorption of Fe^{3+} ion on granular activated carbon has been studied in kinetic and equilibrium conditions taking into account the adsorbate concentration, temperature and solution pH as major influential factors. In addition, the effect of nitrilotriacetic acid on adsorption reaction as a complexing agent has been examined. Kinetic studies showed that the adsorption rate was increased as the initial Fe^{3+} concentration was raised. The adsorption reaction was estimated to be first-order at room temperature. The adsorption rate and equilibrium adsorption of Fe^{3+} increased as the temperature rose. The activation energy for adsorption was approximately $2.23 \, kJ \, mol^{-1}$, which implied that Fe^{3+} mainly physically adsorbed on activated carbon. Coexistence of nitrilotriacetic acid with Fe^{3+} resulted in a decrease of equilibrium adsorption and the extent of decrease was proportional to the concentration of nitrilotriacetic acid. In the presence of nitrilotriacetic acid, the adsorbability of Fe^{3+} decreased with pH. However, the trend was reversed in the absence of nitrilotriacetic acid. When activated carbon was swelled by acetic acid, the specific surface area was increased and maximum swelling was achieved at approximately 48 h of swelling time. Thermodynamic parameters such as ΔG°, ΔH° and ΔS° for adsorption reaction were estimated based on equilibrium data and in connection with these results the thermodynamic aspects of adsorption reaction were discussed.
© 2003 Elsevier B.V. All rights reserved.

Keywords: Adsorption; Ferric ion; Complexing agent; Swelling; Thermodynamic calculation

1. Introduction

Arguably, iron is the most useful and widely used metal in many industries. Iron is an intrinsic component of steel that is used for many industrial materials. In the process of producing iron or manufacturing goods containing iron, much water is needed. As a result,

* Tel.: +82-2-3277-2394; fax: +82-2-3277-3275.
E-mail address: dongsu@mm.ewha.ac.kr (D.S. Kim).

a considerably large amount of wastewater that contains iron is generated as a by-product. That water needs to be treated before discharge.

In general, iron is regarded as one of the essential metal elements for humans. Approximately 3000–5000 mg of iron exists in the human body [1]. Therefore, one can deduce that as long as the quantity of iron in the environment is not too great, it may not be harmful to the human body. However, iron can cause undesirable problems in industrial processes or ecosystems if its concentration in wastewater is not managed properly. For example, the precipitates of iron hydroxide may block pipes and concentrated iron in the water can be accumulated biologically. Also, iron can act as a source material for an unpleasant taste or odor in water. In addition, precipitates of iron form turbidity, which limit the usage of water for drinking or industrial processes. Since iron in the wastewater is able to induce several problems, it has been regarded as one of the major target materials to be removed [2].

In order to control iron content in water, many types of treatment technologies have been utilized, such as precipitation, electrochemical deposition, solvent extraction, ion exchange and adsorption, etc. [3–10]. Precipitation is known to be effective for the treatment of wastewater with a high concentration of iron, but the large amount of sludge produced after treatment may cause side effects. Ion exchange and solvent extraction may be successfully used to reduce the iron concentration to a very low level. However, these processes are known to be very costly. In contrast, adsorption is a cost-effective technique and, is simple to operate. Adsorption usually does not require significant amounts of chemicals and energy and, in some cases, no chemical is needed at all.

The purpose of this study was to investigate the adsorption characteristics of iron(III) ion, which is one of the major elements in iron-containing wastewater, onto granular activated carbon. Activated carbon is known to be very effective for adsorption of heavy metal ions due to its high surface area. Granular form is preferred over powder type because it is easier to handle. The adsorption kinetics of Fe^{3+} have been studied by examining the change in adsorption rate with time for different initial iron concentrations. The effects of pH and temperature on adsorption were also studied and, based on the results, equilibrium characteristics and thermodynamic properties of the adsorption reaction have been estimated.

Another aspect of this study was the examination of the influence of complexing agent on the adsorption reaction since the existence of complexing agents in aqueous system is known to be very influential on the mobilization of heavy metal species that may otherwise be bound to natural particulate matter. Nitrilotriacetic acid (NTA) was chosen as the complexing agent because it is a potential displacer for phosphates, which are contained in most domestic and industrial detergents. Finally, the swelling effect on the surface property of activated carbon was studied, which as swelling most likely allowed the modification of surface area of adsorbent hence anticipating the change in the overall removal efficiency of Fe^{3+}.

2. Materials and methods

2.1. Preparation of adsorbent

Granular activated carbon purchased from Samchulli Co. was ground and sieved to a uniform size range of 710–1000 μm. A N_2 gas adsorption test showed that the average pore

diameter of activated carbon was ca. 1.7 nm and the pore volume was about $0.817\,cm^3\,g^{-1}$. The prepared activated carbon was dried in oven at $100\,^\circ C$ for more than 3 h and stored in a desiccator with silica gel. For the prevention of surface oxidation of adsorbent, an adequate amount of activated carbon for each test was prepared immediately before the experiment and used without delay.

2.2. Specific surface area measurement

Approximately 15 g of activated carbon were placed in a vacuum desiccator (Kartell Inc.) containing diphosphorus pentaoxide (P_2O_5, >97.5% pure, Kanto Chemical Co., Ltd.) and put under a vacuum for more than 1 h to remove moisture from the surface. After weighing the dehydrated adsorbent, an excess amount ethylene glycol monoethyl ether (EGME, 95% pure, Junsei Chemical Co., Ltd.) was applied to the adsorbent to fully wet the surface and vacuum was used again in a desiccator containing calcium chloride ($CaCl_2$, 95% pure, Aldrich Co.) instead of diphosphorus pentaoxide. By plotting the weight of EGME remaining on the adsorbent as a function of vacuum time, the equilibrium weight of EGME for a monolayer coverage was obtained. Subsequently, the specific surface area of activated carbon was estimated using the following equation:

$$A_s = \frac{W_g}{W_s \times 0.000286} \tag{1}$$

where A_s is the specific surface area ($m^2\,g^{-1}$), W_g the weight of EGME remaining on the sample after monolayer equilibration (g), W_s the weight of initial sample dried by diphosphorus pentaoxide (g), 0.000286 the weight of EGME required to form a monolayer on $1\,m^2$ of surface ($g\,m^{-2}$) [11].

2.3. Swelling of activated carbon

Oven dried activated carbon prepared for the adsorption experiment was used for the swelling test with no further treatment. Approximately 250 ml of glacial acetic acid (CH_3COOH, >99% pure, Kanto Chemical Co., Ltd.) were put into a desiccator, which was submerged in a water bath (JEIO TECH Co., Model WB-30D) with the temperature controlled at $60\,^\circ C$. Approximately 1 h was allowed to saturate the inner space of desiccator with acetic acid vapor. Then, approximately 20 g of activated carbon were put in the desiccator and exposed to the vapor. The activated carbon was stirred occasionally to make the swelling even for the entire volume and the carbon's weight was measured according to swelling time. The swollen carbon was dried in an oven at $100\,^\circ C$ for 24 h and cooled in a desiccator with silica gel for the adsorption experiment.

2.4. Adsorption test

2.4.1. Without NTA
To investigate the kinetic aspects of adsorption, adsorption experiments were carried out using 0.5, 1.0, 1.5 and 2.0×10^{-3} M of Fe^{3+} solution at pH 2 varying the adsorption time.

After preparing stock solution by dissolving iron sulfate hexahydrate ($Fe_2(SO_4)_3 \cdot 6H_2O$, >99.9% pure, Showa Chemicals Inc.) in deionized water (18 MΩ), each desired concentration was obtained by diluting this stock solution. Activated carbon (1 g) was put into a 250 ml conical flask containing 50 ml of Fe^{3+} solution and shaken at 20 °C and 200 rpm in a mechanical shaking incubator (Vision Scientific Co., Model KMC-8480) equipped with a temperature controller. To examine the effect of temperature on the adsorption behavior, the temperature of solution (2.0×10^{-3} M, 1 g of activated carbon) was controlled at 20, 30, 40 and 50 °C, respectively. The formation of hydroxide precipitate or complex of ferric ion, effect of pH on adsorption was investigated by changing the pH of the solution (2.0×10^{-3} M) from 2.0 to 3.6 with an interval of 0.3 unit while using 1 g of adsorbent at 20 °C. All equilibrium experiments were performed using 2 h of adsorption as the equilibrium state. The solution pH was adjusted using HCl and NaOH. A shaking speed of 200 rpm was used for both temperature and pH experiments. Adsorption experiments on the swelling effect was conducted at pH 2 and 200 rpm while varying the temperature of the solution (2.0×10^{-3} M). The adsorbed amount of Fe^{3+} on activated carbon was estimated by analyzing the remaining concentration in the solution after separating the activated carbon by centrifuging. The Fe^{3+} concentration was determined by atomic absorption spectrophotometry (AAS, Perkin Elmer, AAnalyst100) at the wavelength of 258 nm and a lamp current of 30 A after diluting the sample to a suitable concentration range if necessary. All experiments were conducted three times and the average results were reported here.

2.4.2. With NTA

The effect of complexing agent on the adsorption characteristics was studied using NTA ($C_6H_9NO_6$, >99% pure, Sigma Chemical Co.) as the ligand. For the Fe^{3+} solution with the concentration of 2.0×10^{-3} M, the influence of pH and temperature on adsorption was determined in the presence of 1.0×10^{-1} M of NTA. To examine the effect of the NTA, its concentration was varied (1.0×10^{-1}, 10^{-2}, 10^{-3} and 10^{-4} M) at pH 2, 20 °C and 200 rpm. All experiments were performed using 1 g of adsorbent and 50 ml of Fe^{3+} solution. The results were compared with those experiments run in the absence of NTA.

3. Results and discussion

3.1. Kinetics of adsorption

Activated carbon adsorption is known to be usually unaffected in its treatment efficiency by temporal qualitative and quantitative changes of pollutants contained in wastewater. Especially, granular activated carbon with a narrow size range was reported to have a high treatment efficiency for wastewater containing a high pollutant concentration [12]. Fig. 1 shows the change in the remaining concentration of Fe^{3+} with different initial concentrations as a function of time. It was observed that adsorption amount increased rapidly at the incipient stage of adsorption and reached almost equilibrium in about 30 min for the investigated range of initial Fe^{3+} concentration. The adsorption amount and rate seemed to increase as the initial adsorbate concentration was raised. This result was in agreement with a previous report which showed that as pH remained constant, the amount of adsorbate
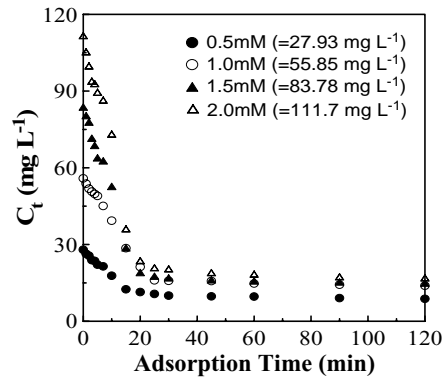
Fig. 1. Change in the remaining concentration of Fe^{3+} according to the adsorption time per unit weight of activated carbon for different initial concentrations of Fe^{3+} (20 °C, pH 2, 1 g activated carbon).

adsorbed onto the surface of adsorbent increased as the initial concentration of adsorbate increased [13]. This phenomenon can be explained by the change of the dispersion force between Fe^{3+} and the surface of activated carbon as adsorption progresses. Since carbon is a non-polar material, the dispersion force will play an important role for interaction between the adsorbate and the activated carbon. In practice, about 95% of the entire surface of a typical activated carbon is considered to be associated with adsorption induced by the dispersion force and the remaining 5% with chemical adsorption [14]. In physical adsorption, polarization of adsorbate can work as part of a driving force for adsorption with no electron transfer [15]. In our case, Fe^{3+} could induce the surface of activated carbon to be slightly negatively charged when it approached the surface of activated carbon and attraction between two dipoles lowered potential energy and eventually brought about adsorption [16].

Variation in the adsorbed amount of Fe^{3+} before reaching equilibrium (Fig. 1), focused on the adsorption time range of 0–10 min, which was discussed kinetically using several forms of kinetic equations; first-order, second-order, and parabolic diffusion. The integrated forms of these kinetic equations are presented in Eqs. (2)–(4) [2,17,18], respectively, and the rate constant for adsorption can be estimated from the slope of the plot of concentration term vs. time

$$\ln\left[\frac{C_t - C_e}{C_0 - C_e}\right] = -kt \tag{2}$$

$$\left[\frac{1}{C_0}\right]\left[\frac{C_0 - C_t}{C_t - C_e}\right] = kt \tag{3}$$

$$\frac{(C_0 - C_t)/(C_t - C_e)}{t} = kt^{1/2} \tag{4}$$

where C_0 is the initial concentration of adsorbate (mg l^{-1}), C_e the equilibrium concentration of adsorbate (mg l^{-1}), C_t the concentration of adsorbate at time, t (mg l^{-1}), t the adsorption time (min), k the reaction rate constant (min^{-1}).
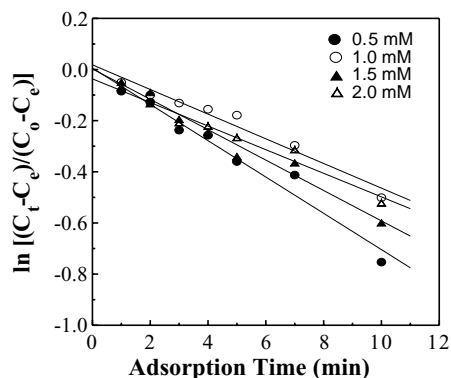
Fig. 2. Linear plots of the first-order kinetic equation for different initial concentrations of adsorbate (20 °C, pH 2, 1 g activated carbon).

A linear plot of the first-order kinetic equation for this system is illustrated in Fig. 2 for different initial concentrations of 0.5, 1.0, 1.5 and 2.0 mM. Reaction rate constants obtained from the slope of each linear plot were calculated to be 0.071, 0.048, 0.059 and 0.046 min^{-1}, respectively, for the initial Fe^{3+} concentrations of 0.5, 1.0, 1.5 and 2.0 mM. The degree of goodness of linear plot between the concentration term vs. time can be judged from the value of the coefficient of determination of the plot, which can also be regarded as a criterion in the determination of the adequacy of kinetic equation. Table 1 summarizes the estimated coefficients of determination for several kinetic model equations in different initial adsorbate concentrations and temperature. From the coefficient of determination values in Table 1, adsorption of Fe^{3+} ion on the activated carbon was regarded as first-order rather than second-order or parabolic diffusion and the reaction characteristics as first-order became more prominent as temperature rose. Especially, for the parabolic diffusion model, which

Table 1

Coefficient of determination for the plots of the time dependence of Fe^{3+} adsorption for several kinetic equations according to the initial concentration and temperature

Kinetic equation	Initial concentration ($\times 10^{-3}$ M)	Coefficient of determination (r^2)	Temperature (°C)	Coefficient of determination (r^2)
First-order	0.5	0.9654	30	0.9720
	1.0	0.9628	40	0.9881
	1.5	0.9726	50	0.9774
	2.0	0.9688		
Second-order	0.5	0.9311	30	0.8728
	1.0	0.9385	40	0.8493
	1.5	0.9102	50	0.8830
	2.0	0.9025		
Parabolic diffusion	0.5	0.7400	30	0.8139
	1.0	0.8521	40	0.4246
	1.5	0.3548	50	0.1438
	2.0	0.8850		

assuming that diffusion of reactants should be the rate-determining step, the linearity of the plots was found to be not good compared with other kinetic models. Therefore, diffusion of Fe^{3+} from bulk solution towards the surface of activated carbon was not considered as the rate-determining step.

In general, the adsorption reaction is known to proceed through the following three steps: (1) transfer of adsorbate from bulk solution to adsorbent surface, which is usually mentioned as diffusion, (2) migration of adsorbate into pores, (3) interaction of adsorbate with available sites on the interior surface of pores [19]. From the previous discussion regarding kinetic aspects of adsorption, it was shown that the parabolic diffusion kinetic model did not explain the adsorption of Fe^{3+} onto the activated carbon well. Thus, diffusion of Fe^{3+} is thought not to be influential on the rate-determining step so that step (1) can be ignored. The pore property of granular activated carbon used in the experiment was found to be approximately 1.7 nm in diameter on average. Considering the ionic radius of Fe^{3+} to be 0.064 nm [20], migration of Fe^{3+} into the micropores of activated carbon can be regarded to easily occur so that step (2) is also not important in the rate-determining of adsorption. Thus, it can be concluded that the rate-determining step for the adsorption of Fe^{3+} ion is step (3).

Along with kinetic consideration, variation of the remaining concentration of Fe^{3+} at equilibrium state was examined by changing the initial concentrations of Fe^{3+}, while keeping the ratio between initial concentration of adsorbate and amount of adsorbent constant. As seen in Fig. 3, the equilibrium adsorption of Fe^{3+} per unit weight of activated carbon increased as the initial concentration of Fe^{3+} and the amount of activated carbon were raised. This phenomenon can be explained in the same way as the kinetics discussion, i.e., since the volume of solution used for each adsorption experiment was the same, the average distance between adsorbate and adsorbent would be reduced as Fe^{3+} concentration was increased. Consequently, the dispersive force between Fe^{3+} ion and surface of activated carbon was more stronger so that more adsorption would take place. At the same time, the increased diffusivity of adsorbate at its higher concentration was also thought to partly contribute to the enhanced adsorption. This observation was considered to be meaningful for the design
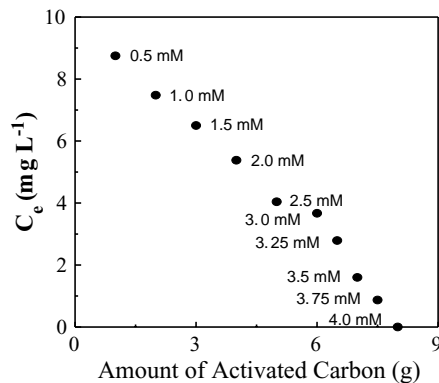

Fig. 3. Variation in the equilibrium concentration of Fe^{3+} according to the initial concentration of adsorbate and the amount of activated carbon maintaining the ratio of two variables as $0.5\,\mathrm{mM\,g^{-1}}$.
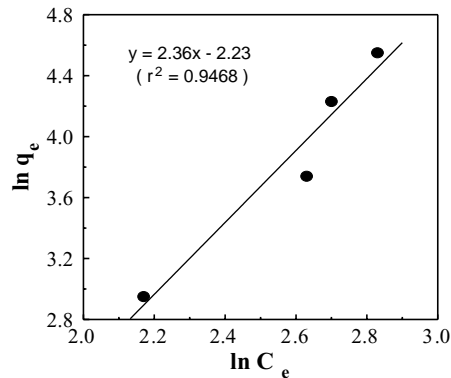
Fig. 4. Freundlich isotherm for the adsorption of Fe^{3+}.

of an optimal operating condition specifically regarding the amount of adsorbent necessary for the efficient treatment of wastewater with changing pollutant concentration.

We attempted to fit the equilibrium data to an adsorption isotherm and found that the equilibrium adsorption of Fe^{3+} on the activated carbon followed the Freundlich isotherm well. The Freundlich model can be expressed as the following equation [21]:

$$q_e = KC_e^{1/n} \tag{5}$$

where q_e is the amount of equilibrium adsorption (mg g^{-1}), C_e the equilibrium concentration of adsorbate (mg l^{-1}), K and $1/n$ are the Freundlich constants related to adsorption capacity and adsorption intensity.

By taking the logarithm for both sides of Eq. (5), linear form of the Freundlich model can be obtained

$$\ln q_e = \ln K + \left(\frac{1}{n}\right) \ln C_e \tag{6}$$

The plot of $\ln q_e$ vs. $\ln C_e$ is given in Fig. 4. It showed good linearity with an r^2 of 0.9468. The values for K and $1/n$ can be obtained from the intercept on y-axis and slope of the linear line. They were estimated to be 0.108 and 2.36, respectively.

3.2. Effect of temperature and pH

The influence of temperature on Fe^{3+} adsorption onto activated carbon was examined and it was observed that although the difference was not great, the adsorption rate and equilibrium adsorption increased slightly as the temperature was increased (Fig. 5). The increase in equilibrium adsorption as the temperature was higher was in accord with previous reports that adsorbed amount of cations at equilibrium was usually observed to be proportional to temperature [22–24]. The kinetics investigation noted previously revealed that the adsorption of Fe^{3+} was first-order even when the temperature was changed (Table 1). The linear plot of the first-order kinetic equation at different temperatures is shown in Fig. 6
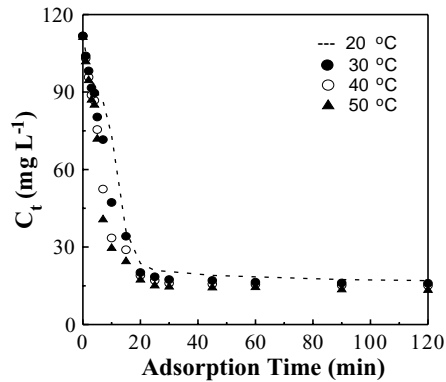
Fig. 5. Change in the remaining concentration of Fe^{3+} according to the adsorption time per unit weight of activated carbon at different temperatures (2.0×10^{-3} M initial concentration, pH 2).

and the rate constants obtained from the slopes of estimated lines were 0.110, 0.175 and 0.201 min^{-1}, respectively, at temperatures of 30, 40 and 50 °C.

It was possible to calculate the activation energy for adsorption based on the result in Fig. 6 employing Arrhenius equation for the rate constant, k [25]

$$k = A \exp\left(-\frac{E_a}{RT}\right) \tag{7}$$

where A is the frequency factor (min^{-1}), E_a the activation energy (kJ mol^{-1}), R the ideal gas constant (kJ mol^{-1} K^{-1}), T the absolute temperature (K).

Eq. (7) can be converted into Eq. (8) by taking logarithm

$$\ln k = \ln A - \frac{E_a}{RT} \tag{8}$$

Thus, E_a could be obtained from the slope of the line plotting $\ln k$ vs. $1/T$ and the estimated E_a for Fe^{3+} adsorption on activated carbon was 2.23 kJ mol^{-1}. Considering that this value
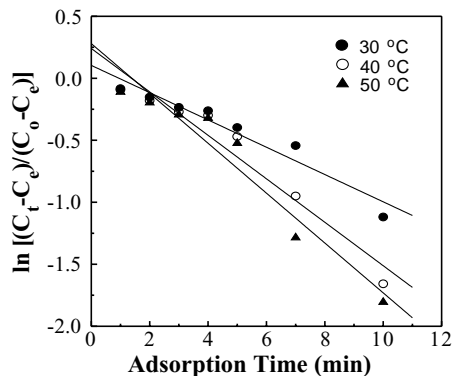

Fig. 6. Linear plots of the first-order kinetic equation for Fe^{3+} adsorption at different temperatures.
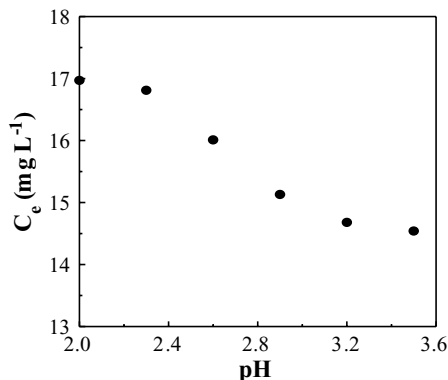
Fig. 7. Effect of pH on the equilibrium concentration of Fe^{3+} (2.0×10^{-3} M initial concentration, 20 °C, 1 g activated carbon).

is in the typical activation energy range for physical adsorption, one can conclude that Fe^{3+} adsorbs on activated carbon mainly physically. This conclusion was also inferred from the dispersive interaction between Fe^{3+} and surface of activated carbon.

One of the most important factors in aquatic systems is pH. In this study, it was expected that surface condition of adsorbent and molecular form of adsorbate were affected by pH. Therefore, the overall adsorption reaction could be governed by this parameter. Fig. 7 shows the change in the remaining concentration of Fe^{3+} at equilibrium state with pH and the equilibrium adsorption increased gradually as pH was raised.

This variation in the adsorbability of ferric ion with pH can be explained by the interaction between hydroxide ion and adsorbent. In general, the stability of the hydroxide ion in solution in its hydrated state is normally lower compared with the proton [26]. This condition results because its ionic radius is larger than that of proton and, therefore, more water molecules are required to surround this ion for hydration. Accordingly, the adsorbability of hydroxide ion on the substrate will be greater than that of proton. When the pH increases, more OH^- will adsorb, making the surface charge of the substrate more negative. As a result, it is expected that the electrostatic attraction between a cationic adsorbate and the substrate becomes stronger and consequently more adsorption will occur. Although not shown here, variation of the electrokinetic potential of fine activated carbon particles prepared from the same granular activated carbon used in the experiment has been examined according to the pH. It was observed that the electrokinetic potential of activated carbon became more negative as the pH increased. This finding verifies the increase in OH^- adsorption with pH from the viewpoint of electrokinetics and explains the increased adsorption of ferric ion.

3.3. Influence of complexing agent

Chemical compounds that form complexes with metal ions usually play an important role in determining the state and mobility of metal ions in aquatic systems. By the same token, it is anticipated that the adsorption features of metal ions will be affected by these compounds when they coexist in solution. In this study, the influence of complexing agent
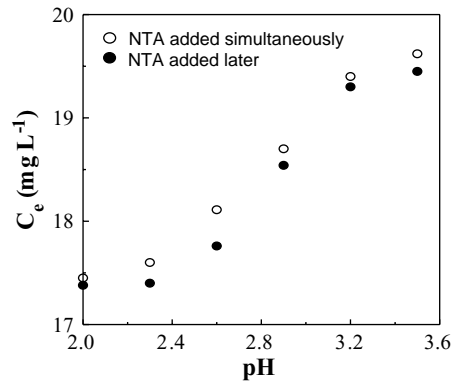
Fig. 8. Effect of NTA (1.0×10^{-1} M) on the equilibrium concentration of Fe^{3+} at different pH's (2.0×10^{-3} M initial concentration, 20 °C, 1 g activated carbon).

on the adsorbability of Fe^{3+} was investigated taking NTA as the ligand. Fig. 8 represents the variations in the equilibrium concentration of Fe^{3+} with pH where NTA was put into the solution simultaneously with Fe^{3+} ions from the beginning. NTA was added to the solution later when the adsorption of Fe^{3+} had reached equilibrium. When this result is compared with experiments conducted with no NTA in solution (Fig. 7), it can be seen that for the case of no NTA, Fe^{3+} adsorbed more as the pH was increased. However, when NTA coexisted with Fe^{3+} the equilibrium adsorption of Fe^{3+} decreased with pH regardless complexing agent was introduced into the solution simultaneously with adsorbate or after equilibrated adsorption was attained. This difference in the adsorption behavior of Fe^{3+} could be explained by the fact that molecular form of NTA is a function of the pH condition.

It is possible to anticipate the predominant form of a certain ionic species depending on the pH in aqueous solution by constructing the pC–pH diagram. The molecular structure of NTA is $(CH_2COOH)_3N$, therefore, it is a triprotonic acid, which dissociates three H^+ ions. The stepwise proton dissociation reactions in solution are as follows:

$$H_3T \Leftrightarrow H_2T^- + H^+ \tag{9}$$

$$H_2T^- \Leftrightarrow HT^{2-} + H^+ \tag{10}$$

$$HT^{2-} \Leftrightarrow T^{3-} + H^+ \tag{11}$$
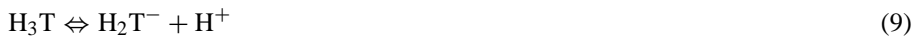
where T denotes $(CH_2COO)_3N$. The total concentration of NTA is expressed as sum of the concentrations of four ionic species

$$C_{total} = [H_3T] + [H_2T^-] + [HT^{2-}] + [T^{3-}] \tag{12}$$

The equilibrium constants for the three reactions (9)–(11) are $10^{-1.66}$, $10^{-2.95}$ and $10^{-10.28}$, respectively [27]. By combining Eqs. (9)–(12), the concentration of each ionic species of NTA can be expressed as a function of C_{total} and $[H^+]$. Considering the experimental concentration of NTA, 1.0×10^{-1} M, the pC–pH diagram for each ionic species for NTA can be constructed (Fig. 9).
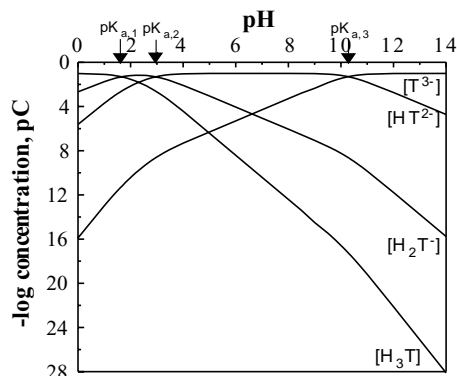
Fig. 9. The pC–pH diagram for 1.0×10^{-1} M NTA solution.

From the pC–pH diagram shown in Fig. 9, it was noted that the predominant ionic form of NTA changed in the order of H_3T, H_2T^-, HT^{2-} and T^{3-} as the pH increased. In general, the extent of complexation between complexing agent and metal cation is enhanced as the negative charge valence of complexing agent increases [28]. Therefore, the Fe^{3+} ion was expected to be combined with NTA and form a complex more strongly as the solution pH became higher. Strong complexation means higher stability of complexes in aqueous environment, which implies less adsorption of metal ions onto the surface of possible substrates.

Fig. 8 also shows that the adsorbability of Fe^{3+} was affected by the manner in which NTA was added to the solution. Namely, Fe^{3+} showed a decreased adsorbability when it coexisted with NTA from the start compared with the case when NTA was added after equilibrium adsorption of Fe^{3+} on activated carbon occurred. The reason for this phenomenon was that the difference in the extent of complexibility of NTA with free Fe^{3+} ion and adsorbed Fe^{3+} on the substrate, i.e., NTA made a complex more easily with Fe^{3+} which exists as a free ion in solution than the one in the adsorbed state. In a practical situation, if some type of complexing agent was introduced into the adsorption process, it would influence the process efficacy via these two mechanisms.

Fig. 10 presents the effect of concentration of NTA on the adsorbability of Fe^{3+} at pH 2. The amount of Fe^{3+} adsorbed decreased as the coexisting amount of NTA from the beginning was raised. This result was understandable in the sense that as the concentration of NTA increased more complexes with Fe^{3+} were expected to form and, consequently, less adsorption of Fe^{3+} occurred.

3.4. Swelling effect

The swelling technique is regarded as a useful method of increasing the surface area of certain solid materials. Swelling equilibrium partly reflects the elastic deformation of the solid surface. This phenomenon is usually induced by an expansion of network structure [28]. Fig. 11 shows the effect of swelling time on the swelling ratio and specific surface area of activated carbon using acetic acid as the swelling solvent. The swelling ratio was
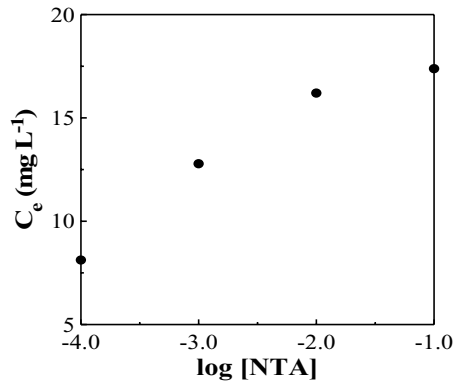
Fig. 10. Change in the equilibrium concentration of Fe^{3+} according to the concentration of NTA (2.0×10^{-3} M initial concentration, 20 °C, pH 2, 1 g activated carbon).

defined as the weight ratio of same sample before and after swelling. As the swelling time increased, the swelling ratio of activated carbon was increased gradually and reached an equilibrium value in approximately 48 h. The specific surface area of the activated carbon also increased with swelling time and became constant after 48 h. Therefore, the changing tendency of the swelling ratio and specific surface area according to the swelling time were very similar to each other. That is, while the amount of acetic acid vapor permeating into the activated carbon increased, the specific surface area of activated carbon also increased. The increase in the specific surface area of activated carbon was due to the fact that during the swelling process a number of fine cracks and micropores were generated on the solid surface by the vaporized solvent, resulting in an increase of the surface area [29]. The observed swelling ratio for activated carbon was much smaller compared than for other solids such as lime, coal, lignite, etc., which were swollen by the same solvent [30,31]. This result was probably due to the original material nature of activated carbon, i.e., when the raw material for activated carbon was activated using proper conditions, its surface area almost reached
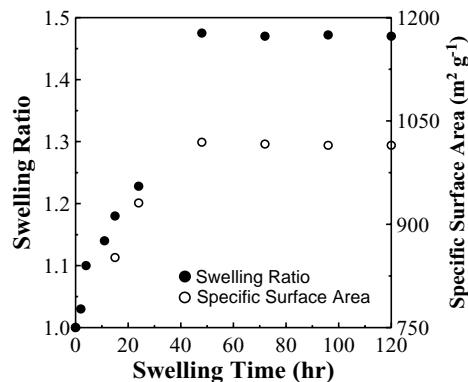

Fig. 11. Variation in the swelling ratio and specific surface area of activated carbon according to the swelling time.
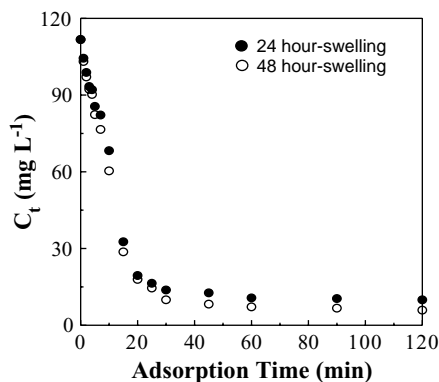
Fig. 12. Variation in the remaining concentration of Fe^{3+} according to the adsorption time per unit weight of swelled activated carbon (2.0×10^{-3} M initial concentration, $20\,^{\circ}$C, pH 2, 1 g activated carbon).

its maximum. Therefore, any additional increase in the surface area by swelling would not be significant.

Fig. 12 illustrates the variation of the remaining concentration of Fe^{3+} with adsorption time when activated carbons swelled for different periods were used as the adsorbent. The experimental condition for adsorption was same as that in Fig. 1 with 2.0×10^{-3} M of initial adsorbate concentration. The adsorption rate and equilibrium adsorption increased compared to the case for non-swelled activated carbon. In addition, as the swelling time increased, more adsorption occurred. Comparison of this result with Fig. 11 revealed that the extent of increase in the equilibrium adsorption of Fe^{3+} was not as much as that in the specific surface area, i.e., although the adsorbed amount of Fe^{3+} increased as the specific surface area of activated carbon became larger as a result of swelling, the extent of the increase for the two parameters were not the same. The reason for this phenomenon was not clear. However, it was thought that the adsorbed amount of adsorbate was determined not only by the surface area of the adsorbent but also by other surface characteristics of the adsorbent and in the course of swelling such surface characteristics of the activated carbon might also be altered along with the change in the specific surface area.

3.5. Thermodynamic aspects of adsorption

To understand the kinetic aspects of the adsorption mechanism of Fe^{3+}, kinetic parameters have been calculated using time course results for different conditions. It was possible to estimate the thermodynamic parameters such as ΔG°, ΔH° and ΔS° for the adsorption reaction by considering the equilibrium constants under the several experimental conditions.

Equilibrium constant for the adsorption reaction of Fe^{3+} on activated carbon, K, was defined as follows:

$$K = \frac{M_{ad}}{C_e} = \frac{C_0 - C_e}{C_e} = \frac{C_0}{C_e} - 1 \tag{13}$$

where M_{ad} is the adsorbed amount of adsorbate at equilibrium, C_0 the initial concentration of adsorbate (mg l^{-1}), C_e the equilibrium concentration of adsorbate (mg l^{-1}).

When the ionic strength effect was considered, the last expression in Eq. (13) changed into $\gamma C_0 / \gamma' C_e - 1$, where γ and γ' represented the activity coefficients of Fe^{3+} ion when the conditions of Fe^{3+} concentration in solution were C_0 and C_e, respectively. Considering the equilibrium results in Fig. 5 and neglecting the adsorption of SO_4^{2-} ion, the ionic strengths of the experimental solution at the initial and equilibrium stage of adsorption were calculated to be 0.030 and about 0.015. Since the differences between C_e's at each temperature in Fig. 5 were not great, the value of 0.015 for ionic strength was an average that was calculated. It assured that no significant error was included. The values for γ and γ' of Fe^{3+} ion for the corresponding ionic strengths were obtained using the extended DeBye–Hückel equation [32]. They were estimated to be 0.3 and 0.4, respectively. As a result, the equilibrium constant could be obtained from the estimated activity coefficients and equilibrium data. All of the equilibrium constants employed in thermodynamic calculations in the present study were obtained by following the same procedure.

The change in the Gibbs free energy for a reaction is expressed as

$$\Delta G = \Delta G^\circ + RT \ln Q \tag{14}$$

here, ΔG° and Q are the standard Gibbs free energy change and reaction quotient, respectively. When the reaction reaches equilibrium state, ΔG becomes zero so that ΔG° is equal to $-RT \ln K$, where K denotes the equilibrium constant. Therefore, ΔG° for an adsorption reaction will be estimated if K for adsorption is known, which can be calculated from the experimental results using Eq. (13). Moreover, using the relationship, $\Delta G^\circ = \Delta H^\circ - T\Delta S^\circ$, $\ln K$ can be expressed in Eq. (15). Thus, if the equilibrium constants for an adsorption reaction at different temperatures are known, the standard enthalpic and entropic changes for adsorption can be also estimated from the slope and intercept of a linear plot of $\ln K$ vs. $1/T$

$$\ln K = -\left(\frac{1}{RT}\right)\Delta H^\circ + \left(\frac{1}{R}\right)\Delta S^\circ \tag{15}$$

Fig. 13 shows the plots of $\ln K$ vs. $1/T$ in different conditions and it can be seen that the linearity of the plots is good.
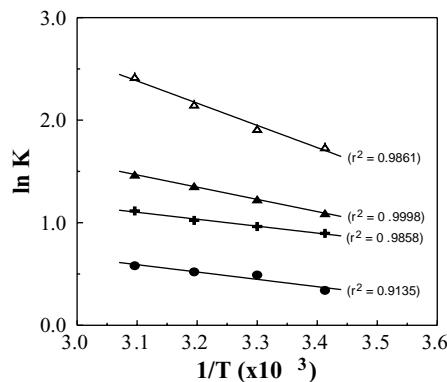

Fig. 13. Linear plots of $\ln K$ vs. $1/T$: ($\triangle$) 48 h-swelling, ($\blacktriangle$) 24 h-swelling, ($+$) no NTA, ($\bullet$) 1.0×10^{-1} M NTA.

Table 2
Thermodynamic parameters of the adsorption reaction of Fe^{3+} onto activated carbon at pH 2

Temperature (°C)	No NTA			1.0×10^{-1} M NTA		
	ΔG° (J mol^{-1})	ΔH° (J mol^{-1})	ΔS° (J K^{-1} mol^{-1})	ΔG° (J mol^{-1})	ΔH° (J mol^{-1})	ΔS° (J K^{-1} mol^{-1})
20	−7790	5.63	26.61	−6840	5.95	23.35
30	−8060	5.63	26.61	−7050	5.95	23.35
40	−8320	5.63	26.61	−7300	5.95	23.35
50	−8590	5.63	26.61	−7540	5.95	23.35
	24 h-swelling			48 h-swelling		
20	−12550	9.90	42.88	−22130	18.00	75.60
30	−12980	9.90	42.88	−22890	18.00	75.60
40	−13410	9.90	42.88	−23650	18.00	75.60
50	−13840	9.90	42.88	−24400	18.00	75.60

Table 2 represents the estimated thermodynamic parameters for Fe^{3+} adsorption in several conditions based on the thermodynamic calculations and results in Fig. 13. It was noted that for all of the considered experimental conditions ΔG° became more negative as the temperature rose and ΔH° had a positive value, which implied that the adsorption reaction of Fe^{3+} was endothermic. Therefore, the experimental results that observed the increase in adsorbability of Fe^{3+} with temperature were substantiated thermodynamically. ΔG° was also estimated to be more negative at the same temperature as the swelling time increased. This condition meant that Fe^{3+} adsorbed more favorably on the activated carbon when swelled for a longer period. In comparison with the cases with and without NTA, ΔG° showed a less negative value when NTA coexisted with Fe^{3+} in solution, therefore, it was understood that the presence of NTA suppressed the adsorption of Fe^{3+} as a result of forming a stable complex with the ferric ion. The positive ΔS°'s for adsorption could be explained by the release of the attached water molecules from Fe^{3+} ion into solution as Fe^{3+} adsorbed on substrate and contributed to the increase in the degree of freedom of the entire system.

4. Conclusions

Studies on the investigation of adsorption features of Fe^{3+} ion on granular activated carbon have been carried out and the influence of NTA as a complexing agent on the adsorption reaction was examined. The following conclusions have been drawn:

1. An increase in the initial concentration of Fe^{3+} resulted in the rise of adsorption rate and equilibrium adsorption, which was considered to be due to the increased dispersive force between Fe^{3+} ion and the surface of the activated carbon. Kinetics investigation showed that the adsorption reaction of Fe^{3+} was first-order and the equilibrium adsorption per unit weight of activated carbon increased as the initial concentration of Fe^{3+} and the amount of adsorbent was enhanced while maintaining the ratio between the two parameters as 0.5 mM g^{-1}.

2. Equilibrium characteristics of an adsorption followed the Freundlich model well. The adsorbability of ferric ion increased with temperature and the estimated activation energy for adsorption substantiated the aspect of physisorption.
3. Equilibrium adsorption was observed to increase as the pH rose. However, when NTA coexisted with Fe^{3+} in solution it decreased with pH. This result could be explained by the variation in the complexibility of NTA with Fe^{3+} ion according to the pH.
4. The adsorbability of Fe^{3+} became lower in proportion to the concentration of NTA. This adsorption was also influenced by the point of time of NTA addition.
5. The specific surface area of activated carbon was increased by swelling, resulting an increase in equilibrium adsorption. The swelling ratio was in proportion to the swelling time and the maximum increase in specific surface area and swelling ratio was achieved in 48 h.
6. It was possible to estimate the ΔG°, ΔH° and ΔS° for the adsorption reaction based on thermodynamic equations and these parameters substantiated the experimental results thermodynamically including the endothermic feature of adsorption.

Acknowledgements

References

[1] W.G. Landis, M.H. Yu, Introduction to Environmental Toxicology, Lewis Publishers, Boca Raton, FL, 1995, p. 130.
[2] G. Bereket, A.Z. Aroguz, M.Z. Ozel, Removal of Pb(II), Cd(II), Cu(II), and Zn(II) from aqueous solutions by adsorption on bentonite, J. Colloid Interf. Sci. 187 (1997) 338.
[3] M. Uchida, S. Ito, N. Kawasaki, T. Nakamura, S. Tanada, Competitive adsorption of chloroform and iron ion onto activated carbon fiber, J. Colloid Interf. Sci. 220 (1999) 406–409.
[4] M. Pakula, S. Biniak, A. Swiatkowski, Chemical and electrochemical studies of interactions between iron(III) ions and activated carbon surface, Langmuir 14 (1998) 3082–3089.
[5] C. Huang, W.P. Cheng, Thermodynamic parameters of iron-cyanide adsorption onto γ-Al_2O_3, J. Colloid Interf. Sci. 188 (1997) 270–274.
[6] M. Kato, S. Kudo, T. Hattori, Adsorption equilibria of 1,10-phenanthroline and its Fe(II) complex on octadecyl-bonded silica gel, Bull. Chem. Soc. Jpn. 49 (1998) 267.
[7] A.G. Belous, E.V. Pashkova, V.A. Elshanskii, V.P. Ivanitskii, Effect of precipitation conditions on the phase composition, particle morphology, and properties of iron(III, II) hydroxide precipitates, Inorg. Mater. 36 (2000) 343–351.
[8] M. Fahlman, H. Guan, J.A.O. Smallfield, A.J. Epstein, The iron/polyaniline interface and its effect on corrosion protection of iron and cold rolled steel in aqueous and salt environments, in: Proceedings of the US Society of Plastics Engineers, ANTEC 1998, Atlanta, GA, May 1998, pp. 1238–1241.
[9] L.A. Voropanova, L.N. Velichko, Extraction of copper(II), nickel(II), cobalt(II), chromium(II), and iron(II, III) ions from aqueous solutions with a technical lubricant, Russ. J. Appl. Chem. 72 (1999) 1970–1975.
[10] M.A. Zarraa, Mass transfer characteristics during the removal of dissolved heavy metals from waste solutions in gas sparged fluidized beds of ion exchange resins, Chem. Eng. Tech. 22 (1999) 533–537.
[11] D.L. Sparks, Environmental Soil Chemistry, Academic Press, San Diego, CA, 1995, p. 42.
[12] W.W. Eckenfelder, Industrial Water Pollution Control, 2nd ed., McGraw-Hill, Singapore, 1989, pp. 263–284.

[13] J.H. Kim, M.H. Sohn, D.S. Kim, S.M. Sohn, Y.S. Kwon, Production of granular activated carbon from waste walnut shell its adsorption characteristics for Cu^{2+} ion, J. Hazard. Mater. 85 (2001) 301–315.

[14] Y. Park, Activated Carbon: Introduction and Application, Donghwa Science Press, Seoul, 1999, p. 30.

[15] D.M. Ruthven, Principles of Adsorption and Adsorption Process, Wiley, New York, 1984, p. 29.

[16] A.W. Adamson, Physical Chemistry of Surfaces, 5th ed., Wiley, New York, 1990, pp. 283–284, 622–623.

[17] J.E. Lee, Adsorption of Pb(II) in the wastewater of natural kaolinite, J. Korean Environ. Sanitation 21 (1995) 77–86.

[18] K.P. Raven, A. Jain, R.H. Loeppert, Arsenite and arsenate adsorption on ferrihydrite: kinetics, equilibrium, and adsorption envelopes, Environ. Sci. Technol. 32 (1998) 344–349.

[19] Y. Onganer, C. Temur, Adsorption dynamics of Fe(III) from aqueous solution onto activated carbon, J. Colloid Interf. Sci. 205 (1998) 241–244.

[20] R.C. Weast, CRC Handbook of Chemistry and Physics, CRC Press, Boca Raton, FL, 1979, p. F-214.

[21] F.A. Banat, B. Al-Bashir, S. Al-Asheh, O. Hayajneh, Adsorption of phenol by bentonite, Environ. Pollut. 107 (2000) 391–398.

[22] B.B. Sahu, H.K. Mishra, K. Parida, Cation exchange and sorption properties of tin(IV) phosphate, J. Colloid Interf. Sci. 225 (2000) 511–519.

[23] M.J. Angove, J.D. Wells, B.B. Johnson, The influence of temperature on the adsorption of cadmium(II) and cobalt(II) on goethite, J. Colloid Interf. Sci. 211 (1999) 281–290.

[24] X. Shile, A.B. Stephen, Cationic surfactant adsorption by swelling and nonswelling layer silicates, Langmuir 11 (1999) 2508–2514.

[25] J.G. Henry, G.W. Heinke, Environmental Science and Engineering, 2nd ed., Prentice-Hall, Englewood Cliffs, NJ, 1996, pp. 193–194.

[26] D.J. Shaw, Introduction to Colloid and Surface Chemistry, 3rd ed., Butterworths, Boston, MA, 1980, p. 140.

[27] S.E. Manahan, Environmental Chemistry, 6th ed., Lewis Publishers, London, 1994, p. 71.

[28] B. Nowack, L. Sigg, Adsorption of EDTA and metal–EDTA complexes onto goethite, J. Colloid Interf. Sci. 177 (1996) 106–121.

[29] N.H. Kim, T.H. See, J.S. Choi, Swelling equilibria of polymeric hydrogels containing poly(acrylamide-sodiumallylsulfonate-acrylic acid), Korean J. Chem. Eng. 17 (2000) 534–540.

[30] Y. Otake, E.M. Suuberg, Solvent swelling rates of low rank coals and implications regarding their structure, Fuel 77 (1998) 901–904.

[31] E. Sasaoka, N. Sada, M.A. Uddin, Preparation of macroporous lime from natural lime by swelling method with acetic acid for high temperature desulfurization, Ind. Eng. Chem. Res. 37 (1998) 3943–3949.

[32] V.L. Snoeyink, D. Jenkins, Water Chemistry, Wiley, New York, 1980, pp. 74–79.